Probing the Role of the F-Helix in Serpin Stability through a Single Tryptophan Substitution†

Lisa D. Cabrita, James C. Whisstock, and Stephen P. Bottomley*

Department of Biochemistry and Molecular Biology, Monash University, P.O. Box 13D, Victoria 3800, Australia

Received October 26, 2001; Revised Manuscript Received January 10, 2002

ABSTRACT: Serpins form loop−sheet polymers through the formation of a partially folded intermediate. Through mutagenesis and biophysical analysis, we have probed the conformational stability of the F-helix, demonstrating that it is almost completely unfolded in the intermediate state. The replacement of Tyr_{160} on the F-helix of α_1-antitrypsin to alanine results in the loss of a conserved hydrogen bond that dramatically reduces the stability of the protein to both heat and solvent denaturation, indicating the importance of Tyr_{160} in the stability of the molecule. The mutation of Tyr_{160} to a tryptophan residue, within a fluorescently silent variant of α_1-antitrypsin, results in a fully active, stable serpin. Fluorescence analysis of the equilibrium unfolding behavior of this variant indicates that the F-helix is highly disrupted in the intermediate conformation. Iodide quenching experiments demonstrate that the tryptophan residue is exposed to a similar extent in both the intermediate and unfolded states. Cumulatively, these data indicate that the F-helix plays an important role in controlling the early conformational changes involved in α_1-antitrypsin unfolding. The implications of these data on both α_1-antitrypsin function and misfolding are discussed.

The misfolding of α_1-antitrypsin (α_1-AT) and other members of the serpin superfamily leads to a variety of disorders (*1*, *2*) such as emphysema, liver cirrhosis (*3*−*6*), thromboembolism (*7*), and dementia (*8*). These disorders arise when the serpin undergoes an inappropriate change in topology that results in self-association and tissue deposition. For example, loop−sheet polymers of α_1-AT have been found in both the liver (*3*) and lung lavage fluid (*9*). These polymers are formed through two related mechanisms. One is due to point mutations that destabilize the native state of the serpin, such that it adopts a partially unfolded conformation with a high propensity to polymerize (*10*−*13*). The second mechanism is that the mutation disturbs the normal folding pathway of α_1-AT, slowing the process down, leading to the accumulation of a partially folded conformation which subsequently polymerizes (*14*). Although it is likely that the partially unfolded conformation adopted during both of these mechanisms is the same, there is no experimental evidence to support this. An essential requirement of elucidating the mechanisms of polymer formation is determining the conformation of intermediates that populate the normal (un)folding pathway of the protein.

The native conformation of α_1-AT and other members of the serpin superfamily is metastable (*15*). In the metastable state the A β-sheet consists of five strands, whereas in the more stable latent or cleaved conformations the A β-sheet has six strands. The ability of the serpin scaffold to adopt these more stable conformations is essential for proteinase inhibition. Once the proteinase docks onto the reactive center loop (RCL) of the serpin, it initiates cleavage of the scissile bond, between the $P_1-P_{1'}$ residues. Cleavage progresses as far as the acyl-enzyme intermediate, where the proteinase is covalently attached to the P_1 residue and the $P_1-P_{1'}$ bond is broken (*16*). Cleavage of the $P_1-P_{1'}$ bond enables the serpin to undergo the native to cleaved transition, resulting in the proteinase being translocated to the opposite pole of the molecule (*17*). This results in the proteinase becoming distorted and trapped in an intermediate conformation, unable to complete its cleavage reaction (*17*−*20*). This remarkable mechanism, in which the A β-sheet opens up and accepts its own RCL residues, renders the serpin architecture sensitive to mutations that cause inappropriate conformational change (*1*). It is proposed that mutations enhance or stabilize an expanded A β-sheet, resulting in insertion of the RCL from another serpin molecule and the formation of loop−sheet polymers. These polymers go on to form long chains and deposit within various tissues.

Understanding the conformational changes involved in serpin folding and unfolding is critical to our understanding of serpin-related disease. Previous data suggest that α_1-AT unfolds through one intermediate conformation; however, little is known about the conformation of this state (*12*, *21*−*23*). Recently, biochemical and crystallographic data have suggested that the F-helix, which lies on top of the A β-sheet, plays a fundamental role in serpin function and dysfunction (*24*−*29*). On the basis of their crystallographic data Gooptu et al. (*27*) proposed that the F-helix can act as a "shoe horn" to open the A β-sheet during both folding and inhibitory pathways. As part of our ongoing analysis of the conformational changes involved in α_1-AT folding, we have placed a unique tryptophan residue on the F-helix to examine the stability and role of this region. The presence of this reporter group has allowed insight into the structure of a partially folded intermediate, which has implications in both serpin folding and misfolding.

† This work was supported by grants from the National Health and Medical Research Council and the Australian Research Council to S.P.B. S.P.B. is a Logan Fellow.

* Corresponding author. Tel: (61)-3-99053703. Fax: (61)-3-99054699. E-mail: steve.bottomley@med.monash.edu.au.

10.1021/bi0158932 CCC: $22.00
Published on Web 03/13/2002

MATERIALS AND METHODS

Production and Characterization of α_1-AT. The first variant created was α_1-AT$_{(Y160A)}$ in which tyrosine 160 was replaced by an alanine; this was made using α_1-AT (P1 = Arg) as the template which contains both of its native tryptophan residues. Tyrosine 160 was also mutated to a tryptophan residue to create α_1-AT$_{(Y160W)}$. This was performed using α_1-AT$_{(FF)}$ as the template where the P_1 = Arg and Trp$_{194}$ and Trp$_{238}$ have both been replaced by phenylalanine (*19*). Both mutations were made using the QuikChange site-directed mutagenesis kit (Stratagene) and verified with DNA sequencing. The proteins were expressed in *Escherichia coli* and purified as previously described (*30*).

Determination of the Stoichiometry of Inhibition and Rates of Inhibition. The stoichiometry of inhibition (SI) and the association rate constant (k_{assoc}) between thrombin and the antitrypsin variants were determined at 37 °C as previously described (*31*).

Production and Characterization of Thrombin. Thrombin was purified from human plasma and characterized as previously described (*32*).

Spectroscopic Methods. Fluorescence emission spectra were recorded on a Perkin-Elmer LS50B spectrofluorometer at 25 °C in a 1 cm path-length quartz cell. Excitation and emission slits were set at 2.5 nm for all spectra, and a scan speed of 10 nm/min was used. The absorbance at the excitation wavelength was monitored in all experiments and remained below 0.05. Circular dichroism spectra were measured on a Jasco 810 spectropolarimeter at 25 °C. Far-UV spectra from 190 to 250 nm were collected with 5 s/point signal averaging; θ_{222} measurements were made with the signal averaged over 15 s. The concentration of protein used was 0.1 mg/mL with a 0.1 cm path length.

Gel Electrophoresis. Native PAGE was performed using a method modified from that of Goldenberg as previously described (*33*).

Chemical Denaturation. Stock solutions of guanidine hydrochloride (GdnHCl) in 50 mM Tris and 50 mM NaCl, pH 7.8, were prepared and filtered through 0.22 μm membranes before use. The GdnHCl concentration was determined by refractive index measurements as previously described (*34*). Equilibrium unfolding and refolding curves were determined by adding a concentrated solution of either native or denatured protein to a series of GdnHCl concentrations. These solutions were incubated for 2 h at 25 °C before analysis by measuring either the fluorescence emission spectra of the protein solution or the change in signal at 222 nm in the far-UV spectra, as a function of denaturant concentration. No differences were observed in experiments where spectroscopic measurements were made after more extensive equilibration.

Equilibrium Unfolding Analysis. All GdnHCl unfolding curves were found to be fully reversible, as previously observed (*12*, *35*), and the data were fit to either a two- or three-state unfolding model, using a nonlinear least-squares fitting algorithm, as previously described (*36*−*38*). The three-state analysis recognizes the presence of one stable intermediate structure, I, populated during the transition from the folded state (N) to the unfolded state (U). The free energy of unfolding in 0 M denaturant, ΔG_{H_2O}, and the *m* value, which reflects the sensitivity of ΔG to the GdnHCl concentration, for each transition were determined from this analysis. The midpoint, D_m, of each transition was calculated by $\Delta G_{H_2O}/m$.

Fluorescence Quenching Experiments. Fluorescence quenching measurements were performed in 50 mM Tris, pH 7.8, at different concentrations of GdnHCl. Aliquots of KI (2 M stock) containing 1 mM $Na_2S_2O_3$ were added to protein solutions, and the change in fluorescence emission intensity of the tryptophan residues (λ_{ex} = 290 nm) was measured. Measurements in the presence of denaturant were made on individual samples so there was no dilution of the GdnHCl. The data were analyzed as previously described by Lehrer (*39*). All data were corrected for inner filter effects where necessary.

RESULTS AND DISCUSSION

Importance of Tyrosine 160 to Serpin Stability and Function. All of the inhibitory members of the serpin superfamily can undergo many forms of conformational change (*17*, *40*−*42*). The initial aim of this work was to gain insight into the conformational changes that occur specifically within the F-helix as α_1-AT folds and unfolds. The structural changes involved in this process are important in our understanding of α_1-AT function, misfolding, and polymer formation. Initially, we chose to remove interactions between the F-helix and the A β-sheet to examine the effect this would have on the function and stability of α_1-AT, as we hypothesized that these interactions are critical in maintaining serpin structure and function. The side chain of Tyr$_{160}$ forms a hydrogen bond between its hydroxyl group and Glu$_{141}$, which is situated on the first strand of the A β-sheet (Figure 1). This hydrogen bond is present in most inhibitory serpins (*43*). Analysis of the X-ray crystal structure of native α_1-AT (*44*) reveals that Tyr$_{160}$ lies approximately two-thirds of the way up the F-helix, in the center of a loosely packed pocket formed by Phe$_{119}$ (s2A), Glu$_{141}$ (s1A), Phe$_{143}$ (s1A), Ile$_{157}$ (hF), Val$_{185}$ (s3A), and Tyr$_{187}$ (s3A) (Figure 1). Comparison of the X-ray crystal structures of native, cleaved, and proteinase-bound α_1-AT revealed that this region undergoes limited rearrangement upon transition to the cleaved or proteinase-bound states and that the hydrogen bond is maintained in all conformations (*17*, *45*).

To assess the importance of Tyr$_{160}$, we made two variants. First, we replaced Tyr$_{160}$ with an alanine (α_1-AT$_{(Y160A)}$) to remove the hydrogen bond between this residue and the A β-sheet, and second, a tryptophan residue was introduced (α_1-AT$_{(Y160W)}$) to allow the site-specific monitoring of conformational change. The α_1-AT$_{(Y160A)}$ variant possessed both native tryptophan residues (194 and 238), while α_1-AT$_{(Y160W)}$ has only the single tryptophan in position 160 as it was constructed using α_1-AT$_{(FF)}$ as the template where both Trp$_{194}$ and Trp$_{238}$ have been replaced by phenylalanine (*19*). Tryptophan is commonly found at position 160 in many serpin members (*43*), and we predict that the hydrogen bond to Glu$_{141}$ is maintained in α_1-AT$_{(Y160W)}$, as examination of the X-ray crystal structure of active serpin 1K [PDB identifier 1SEK (*46*)] reveals that it is possible for Trp$_{148}$ (equivalent to Tyr$_{160}$) on the F-helix to form a side chain hydrogen bond to Glu$_{129}$ (equivalent to Glu$_{141}$).

The SI and k_{assoc} for α_1-AT$_{(Y160W)}$ were determined against thrombin and were similar to the wild type with values of

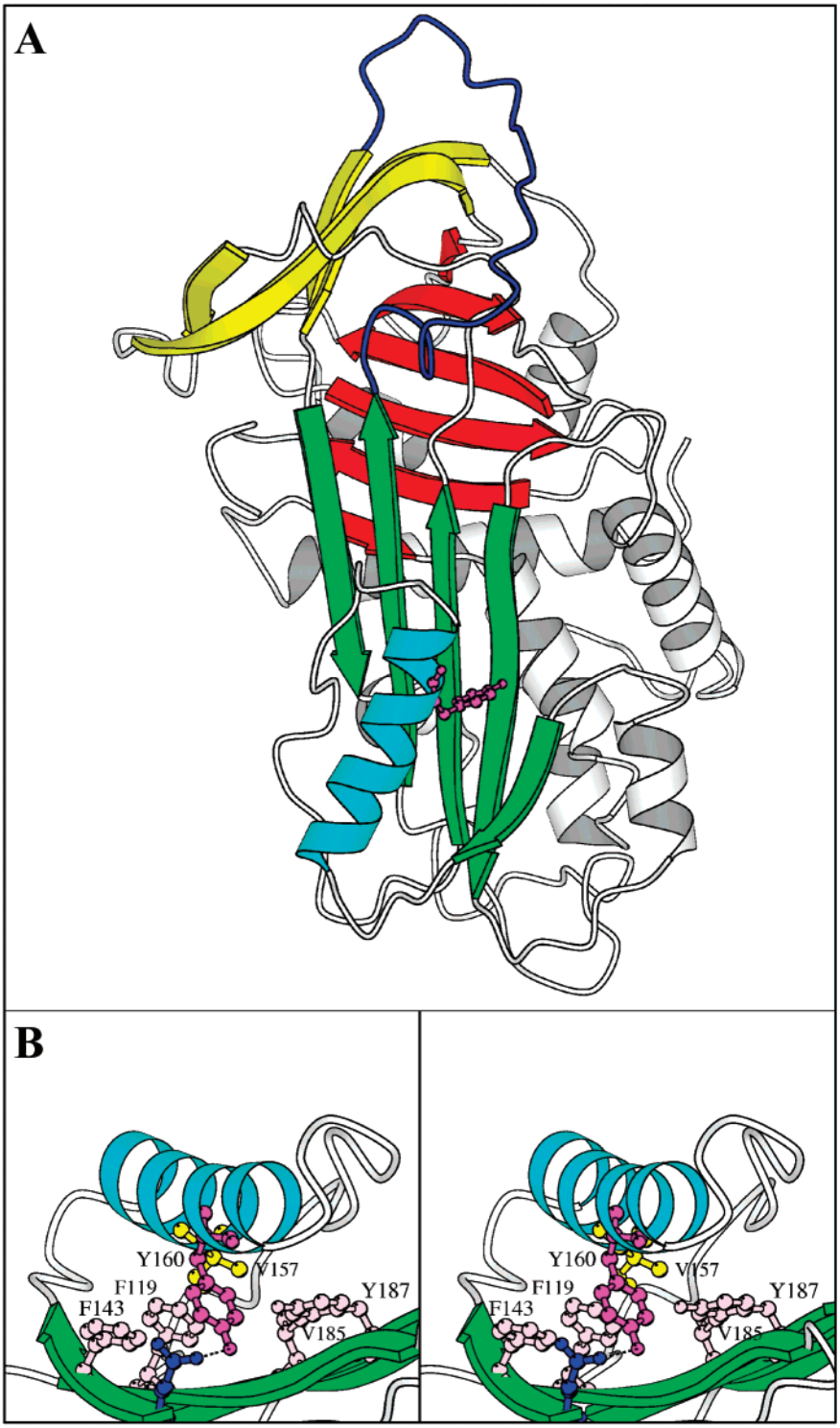

FIGURE 1: Schematic diagram of native α_1-AT. (A) Native α_1-AT with the three β-sheets highlighted (A, green; B, red; and C, yellow). The RCL is in dark blue and the F-helix is in light blue; Tyr_{160} is shown in ball and stick format. (B) Stereo diagram showing the residues on the A β-sheet (green) in close contact with Tyr_{160} (pink). The hydrogen bond between Tyr_{160} and Glu_{141} (purple) is highlighted. This figure was produced using Molscript (*59*).

1.1 ± 0.1 and 4.6×10^5 M^{-1} s^{-1}, respectively (Figure 2, Table 1), whereas the SI and k_{assoc} for α_1-$AT_{(Y160A)}$ were both significantly changed at 6.5 ± 0.2 and 6.2×10^3 M^{-1} s^{-1}, respectively (Table 1). Figure 2 shows SDS−PAGE analysis of the reaction products between α_1-$AT_{(Y160A)}$ and thrombin, confirming the partial substrate nature of α_1-$AT_{(Y160A)}$.

The thermal stability of α_1-$AT_{(Y160A)}$ and α_1-$AT_{(Y160W)}$ was assessed by far-UV CD and nondenaturing PAGE. The midpoint of the thermal unfolding, as determined using far-UV CD, for α_1-$AT_{(Y160A)}$ was 54 °C (Figure 3A; Table 1), 5 °C lower than wild-type α_1-AT (59 °C). In contrast, the midpoint of the thermal transition was determined to be 65 °C for α_1-$AT_{(Y160W)}$, an increase of 7 °C compared to α_1-$AT_{(FF)}$ (58 °C) (*19*). To assess whether the mutations affected the polymerization properties of the molecules, α_1-AT and the two variants were heated at 60 °C over a 30 min period, during which aliquots were collected and placed directly on ice to quench further polymerization. Nondena-

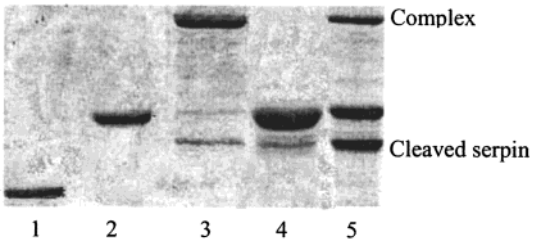

FIGURE 2: SDS−PAGE analysis of the interaction between the F-helix variants and thrombin. Thrombin (lane 1) and both α_1-AT$_{(Y160W)}$ (lane 2) and α_1-AT$_{(Y160A)}$ (lane 4) were incubated together for 30 min at an enzyme to inhibitor ratio of 1:2 and 1:10, respectively. The products of the reaction were then run on a 12% SDS−PAGE (lane 3, α_1-AT$_{(Y160W)}$ + thrombin; lane 5, α_1-AT$_{(Y160A)}$ + thrombin).

Table 1: Inhibitory and Stability Properties of α_1-AT and Tryptophan Mutants[a]

	SI	k_{assoc} (M^{-1} s^{-1})	T_m (°C)
α_1-AT	1.0 ± 0.1	4.8×10^5	59 ± 0.2
α_1-AT$_{(FF)}$[b]	1.1 ± 0.1	6.0×10^5	58 ± 0.2
α_1-AT$_{(Y160A)}$	6.5 ± 0.2	6.2×10^3	54 ± 0.1
α_1-AT$_{(Y160W)}$	1.1 ± 0.1	4.6×10^5	65 ± 0.2

[a] The SI and k_{assoc} were determined against thrombin as described in Materials and Methods. All estimates of k_{assoc} have standard errors less than 5%. The T_m was determined using far-UV CD and represents the average of three separate determinations. [b]Reference *19*.

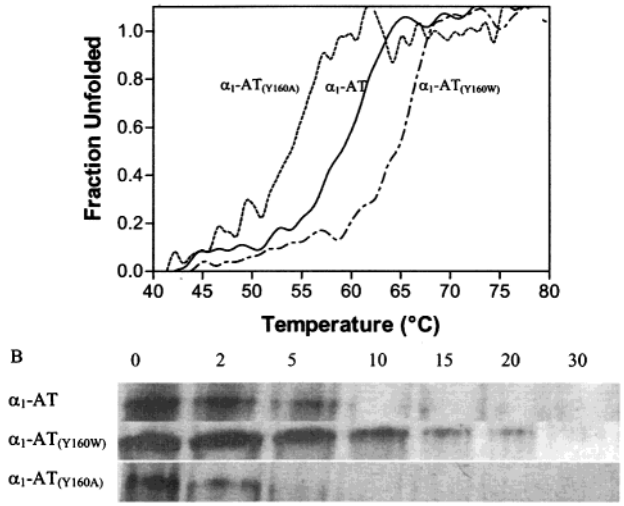

FIGURE 3: Thermal denaturation of α_1-AT. (A) The thermal unfolding of (—) α_1-AT, (- − -) α_1-AT$_{(Y160W)}$, and (---) α_1-AT$_{(Y160A)}$ was followed using changes in the far-UV CD at 222 nm. The temperature was increased at a rate of 1 deg/min. The data are plotted as the fraction unfolded against temperature. (B) α_1-AT, α_1-AT$_{(Y160W)}$, and α_1-AT$_{(Y160A)}$ were heated at 60 °C, and aliquots were removed at the times indicated (min) and immediately added to ice-cold nondenaturing loading buffer prior to electrophoresis. This figure shows the change in monomer concentration as the reaction proceeds.

turing gel analysis of the products indicated that α_1-AT polymerized within 10 min, as judged by the loss of monomeric material (Figure 3B). In keeping with the far-UV CD data, α_1-AT$_{(Y160W)}$ was more stable, and monomeric protein was present for approximately 20 min (Figure 3B). α_1-AT$_{(Y160A)}$ was far less stable and polymerized within 5 min (Figure 3B). To our knowledge α_1-AT$_{(Y160W)}$ displays the biggest increase in stability observed for a single substitution within α_1-AT; the Phe$_{51}$Leu mutation resulted

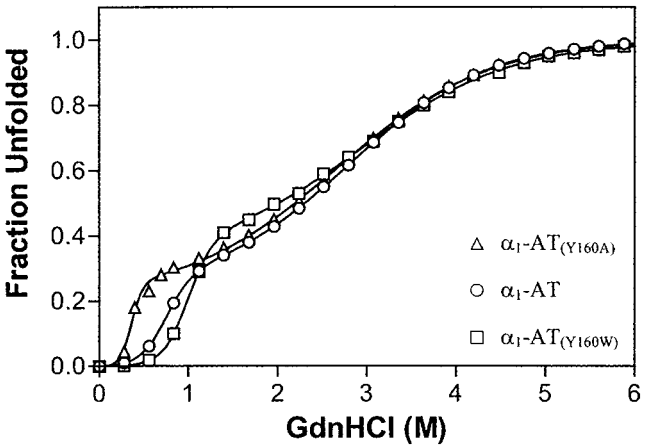

FIGURE 4: Far-UV CD unfolding profile of α_1-AT. The unfolding of (○) α_1-AT, (□) α_1-AT$_{(Y160W)}$, and (△) α_1-AT$_{(Y160A)}$ was followed by far-UV CD at 222 nm. The raw CD data were converted to plots of fraction unfolded as previously described (*60*).

in an increase of 4 °C (*13*). We propose that the increased size of the Trp side chain is the critical determinant behind the increase in stability and that this residue is able to pack more effectively into the surface pocket. This would "lock" the F-helix to the A-sheet and delay expansion of the A β-sheet, which is the first step in both solvent and thermal denaturation (*12*, *13*, *47*). The data with α_1-AT$_{(Y160A)}$ are consistent with this hypothesis; the Ala side chain will not be able to form the hydrogen bond to Glu$_{141}$, and in addition, the small size of the Ala side chain will leave a "hole" in the pocket, which would be energetically unfavorable, hence the decreased stability.

Equilibrium Folding Studies. The unfolding pathway of α_1-AT is best described by N ↔ I ↔ U (*12*, *35*). Far-UV CD analysis of α_1-AT$_{(Y160A)}$ and α_1-AT$_{(Y160W)}$ unfolding reveals that both proteins undergo a three-state unfolding reaction. α_1-AT$_{(Y160A)}$ has two transitions centered around 0.43 and 2.9 M GdnHCl (Figure 4, Table 2). The N to I transition occurred at a GdnHCl concentration 0.4 M lower than that observed for α_1-AT while the second transition was unchanged, demonstrating that the interactions that Tyr$_{160}$ forms are important in stabilizing only the native state of the serpin and not the intermediate conformation. α_1-AT$_{(Y160W)}$ undergoes a similar three-state transition (Figure 4); however, the N to I transition occurs at a higher GdnHCl concentration of 1.0 M, compared to the same transition for α_1-AT at 0.7 M (Figure 4, Table 2). This intermediate then unfolds to give the denatured state; the midpoint of the I to U transition is 2.9 M GdnHCl, which is similar to α_1-AT, 2.8 M (Table 2). The shift in midpoint for the N to I transition is consistent with the thermal denaturation data, indicating that the Trp residue forms additional stabilizing interactions in the native state.

When the unfolding of α_1-AT$_{(Y160A)}$ was monitored by fluorescence intensity, two transitions were observed, a small increase followed by a larger decrease, and the midpoints of these matched well with those observed by far-UV CD, 0.5 and 2.8 M GdnHCl, respectively (Figure 6, Table 2). The changes in λ_{max} followed a two-state process, describing the intermediate to unfolded transition similar to α_1-AT (*12*). The midpoint for this transition agreed well with the second transition observed with far-UV CD at 2.9 M GdnHCl (Figure 6).

Table 2: Equilibrium Unfolding Data[a]

	Three-State Analysis					
	$\Delta G_{N\rightarrow I}$ (kcal/mol)	$m_{N\rightarrow I}$ (kcal mol^{-1} M^{-1})	$D_{mN\rightarrow I}$ (M)	$\Delta G_{I\rightarrow U}$ (kcal/mol)	$m_{I\rightarrow U}$ (kcal mol^{-1} M^{-1})	$D_{mI\rightarrow U}$ (M)
fluorescence int$_{330}$						
α_1-AT	4.8	5.4	0.9	3.2	1.1	2.9
α_1-AT$_{(Y160W)}$	4.75	6.0	0.8	2.5	1.1	2.3
α_1-AT$_{(Y160A)}$	4.3	7.9	0.5	2.4	0.83	2.9
fluorescence λ_{max}						
α_1-AT$_{(Y160W)}$	3.3	3.8	0.9	3.01	1.39	2.17
far-UV CD						
α_1-AT	2.9	3.9	0.74	2.1	0.76	2.8
α_1-AT$_{(Y160W)}$	4.2	4.2	1.0	2.0	0.70	2.9
α_1-AT$_{(Y160A)}$	2.8	6.4	0.43	2.0	0.71	2.8

	Two-State Analysis		
	$\Delta G_{N\rightarrow U}$ (kcal/mol)	$m_{N\rightarrow U}$ (kcal mol^{-1} M^{-1})	D_m (M)
fluorescence λ_{max}			
α_1-AT	2.2	0.8	2.8
α_1-AT$_{(Y160A)}$	2.6	0.9	2.9

[a] Results from Figures 4 and 6 were fit to either a two- or three-state unfolding analysis as described in Materials and Methods; the results presented are the average of five individual curves. $\Delta G_{N\rightarrow I}$ and $\Delta G_{I\rightarrow U}$ represent the free energy change for the unfolding for the N → I and I → U transitions, respectively. $m_{N\rightarrow I}$ and $m_{I\rightarrow U}$ represent the *m* values for the N → I and I → U transitions, respectively. $D_{mN\rightarrow I}$ and $D_{mI\rightarrow U}$ represent the midpoint of denaturation for the N → I and I → U transitions, respectively.

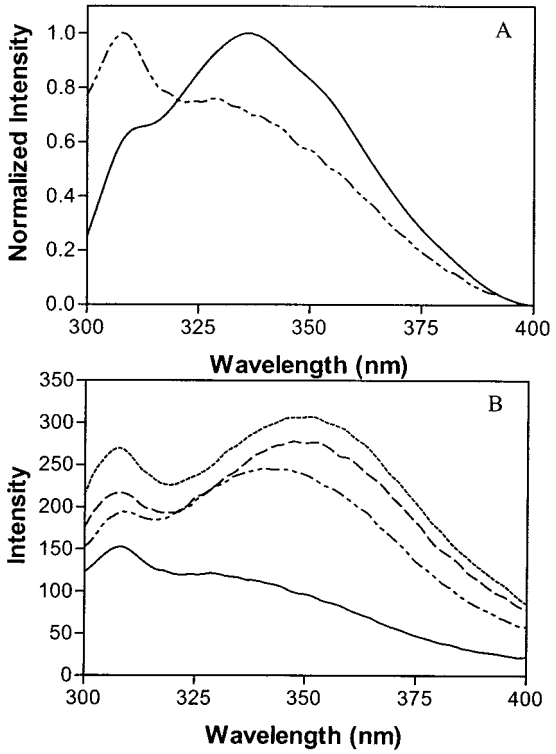

FIGURE 5: Fuorescence emission spectra for α_1-AT and α_1-AT$_{(Y160W)}$. (A) Normalized emission spectra (λ_{ex} = 290 nm) of native (—) α_1-AT and (-- — --) α_1-AT$_{(Y160W)}$. (B) Change in emission spectra of α_1-AT$_{(Y160W)}$ with increasing denaturant concentrations: (—) 0 M through (---) 6 M GdnHCl. All spectra were recorded using a band-pass of 2.5 nm at a temperature of 25 °C.

The replacement of the two native tryptophan residues within α_1-AT$_{(Y160W)}$ with phenylalanine and the incorporation of a unique tryptophan residue afford the protein's different spectroscopic properties. The emission maxima of α_1-AT$_{(Y160W)}$ was blue shifted relative to the wild type by 4 nm to 332 nm (Figure 5A). The fluorescence emission intensity was also heavily quenched, and there is a significant tyrosine shoulder compared to the wild type, indicative of a buried residue (*48*). This quenching is released upon complete unfolding with the fluorescence intensity of α_1-AT$_{(Y160W)}$, increasing more than 3-fold compared to its native state (Figure 5B).

The incorporation of a single fluorescent reporter group permits the site-specific monitoring of conformational changes (*23*, *49*−*53*). The equilibrium unfolding pathway of α_1-AT$_{(Y160W)}$ was followed using both changes in fluorescence intensity at 330 nm and λ_{max} with increasing GdnHCl concentration (Figure 6C). Both sets of data indicate the presence of one intermediate, in 1.2 M GdnHCl, similar to that observed by far-UV CD. The fluorescence intensity data have a short pretransition baseline followed by an increase at low GdnHCl concentration to a maximum at 1.2 M, where the intermediate state is populated, followed by a smaller intensity decrease as the protein fully unfolds. The changes in λ_{max} are similar. The first transition (0.5−1.2 M GdnHCl) is characterized by a large shift in emission maximum from 334 to 345 nm in the intermediate state, indicative of a solvent-exposed tryptophan residue. In the second transition (1.4−3.0 M GdnHCl) there is only a small shift in emission maximum from 345 to 350 nm, indicating full solvation of the exposed tryptophan residue. The midpoints of the second transition are at 2.3 M (intensity) and 2.17 M (λ_{max}); these are 0.6 M lower than the midpoint determined from far-UV CD. Due to the far-UV CD unfolding behavior of the wild type and α_1-AT$_{(Y160W)}$ being extremely similar, it is unlikely that this difference is due to changes in the unfolding characteristics of the protein (Figure 4). Rather, we propose that the single tryptophan residue is reporting the presence of an additional intermediate. This is in keeping with other serpin folding studies on antithrombin (*54*) and antichymotrypsin (*35*) where at least two unfolding intermediates were observed. Taken together, our data demonstrate that upon formation of the first intermediate there is a significant conformational change within the F-helix region in which the tryptophan residue becomes highly solvent exposed.

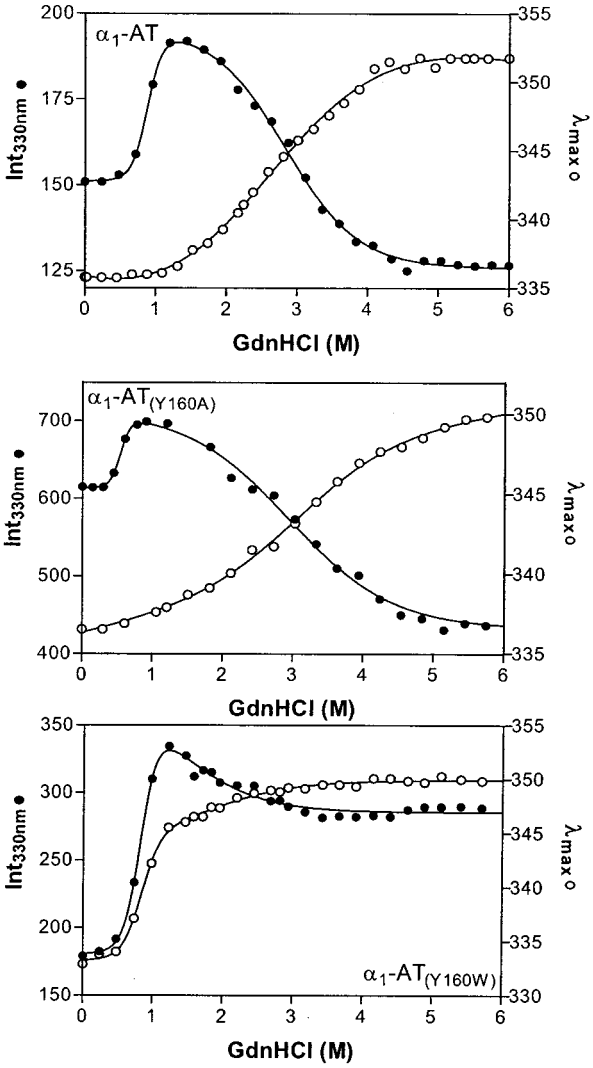

FIGURE 6: GdnHCl-induced equilibrium unfolding of α_1-AT. Structural changes in (A) α_1-AT, (B) α_1-AT$_{(Y160A)}$ and (C) α_1-AT$_{(Y160W)}$ during unfolding were monitored using either changes in fluorescence intensity (●) or emission maxima (○). All experiments were performed at 25 °C with a 2.5 nm band-pass and λ_{ex} = 290 nm.

The conformation of the F-helix during equilibrium unfolding was further characterized by fluorescence quenching experiments. This technique measures the accessibility of a nonfluorescent quenching agent such as iodide to the fluorescence group, providing a sensitive means of characterizing the structure of the intermediate. Various amounts of iodide were added to the native (0 M GdnHCl), intermediate (formed in 1.5 M GdnHCl), and unfolded (6 M GdnHCl) states of α_1-AT$_{(Y160W)}$, and the changes in fluorescence emission intensity from the single tryptophan residue were monitored. The Stern−Volmer plot was linear over the concentration range studied (Figure 7). At 1.5 M GdnHCl the tryptophan residue became far more accessible to iodide than in the native state with an almost 2-fold increase in K_{SV}. In accord with the unfolding data there was little difference in the K_{SV} value determined for the intermediate and unfolded conformations. These data further indicate that the F-helix is grossly disrupted in the intermediate conformation.

The conformation of the first intermediate has previously been examined using fluorescent probes, and it was shown that the top of the A β-sheet was distorted (*12*, *23*). Taken

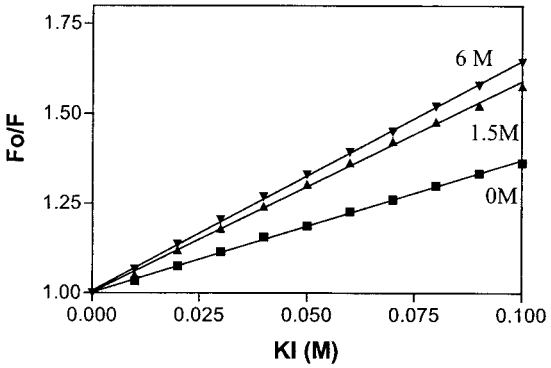

FIGURE 7: Stern−Volmer plot for iodide quenching of α_1-AT$_{(Y160W)}$. Solutions of α_1-AT$_{(Y160W)}$ in buffer (■) and 1.5 M (▲) and 6 M (▼) GdnHCl were incubated with increasing amounts of KI, and the fluorescence emission intensity (λ_{ex} = 290 nm; λ_{em} = 332 nm) was recorded. The lines represent a least-squares fit of the experimental data as described previously (*39*). The K_{SV} values were determined to be 3.7 ± 0.04, 5.9 ± 0.07, and 6.3 ± 0.05 M^{-1} for the protein in 0, 1.5, and 6 M GdnHCl, respectively.

together, our data suggest that opening of the A β-sheet induces a substantial conformational change in the F-helix, whichis linked via a loop from its C-terminus to the A β-sheet. The recent crystal structure of the δ form of antichymotrypsin supports the hypothesis that conformational change in the F-helix is linked to opening of the A β-sheet. In the δ form the C-terminal portion of the F-helix partially unfolds and forms part of the A β-sheet, while the top of the A β-sheet expands to allow insertion of some RCL residues (*27*).

Implications for the Serpin Inhibitory and Polymerization Pathways. Both serpin inhibitory function and misfolding involve the insertion of RCL residues into either their own A β-sheet or the A β-sheet of another molecule. It can clearly be seen from Figure 1 that the F-helix acts as a physical barrier to the rapid insertion of the RCL when a proteinase is attached. Similarly, recent crystal structures and biophysical data indicate that during polymerization the RCL residues from another molecule insert into the lower half of the A β-sheet, which is obscured by the F-helix (*40*, *41*, *55*).

Carrell and colleagues recently proposed that the proteinase partially denatures once inhibited by the serpin and that this aids the conformational transition past the F-helix (*17*). Our data suggest that the F-helix itself may undergo an unfolding/folding reaction that facilitates the rapid movement of the proteinase from the top of the serpin to the bottom. The available kinetic and structural data suggest that the transition from the docking complex to the acyl intermediate involves partial insertion of the RCL into the A β-sheet (*56*−*58*). This opening of the A β-sheet would result in a significant conformational change in the F-helix that would facilitate the full transition of the proteinase to the opposite pole.

Serpin polymerization can occur via two pathways: either by partial unfolding of the native state or during folding to the native state (*3*−*6*, *14*). Biophysical evidence suggests that partial unfolding of the serpin results in an expanded A β-sheet (*11*−*14*, *47*). Our data indicate that this would cause the F-helix to partially unfold, leaving the way open for RCL insertion in the bottom half of the A β-sheet.

Serpins represent a family of proteins with the ability to undergo conformational change. The molecular mechanisms of these changes are important to understanding the regula-

tion of many biological processes and the cause of numerous diseases. Our data indicate that the F-helix is conformationally labile and plays a fundamental role in controlling serpin conformational changes.

ACKNOWLEDGMENT

We thank Dr. Carla Chinni and members of the laboratory for advice and helpful discussions.

REFERENCES

1. Stein, P. E., and Carrell, R. W. (1995) *Nat. Struct. Biol. 2*, 96−113.
2. Carrell, R. W., and Gooptu, B. (1998) *Curr. Opin. Struct. Biol. 8*, 799−809.
3. Lomas, D. A., Evans, D. L., Finch, J. T., and Carrell, R. W. (1992) *Nature 357*, 605−607.
4. Lomas, D. A., Evans, D. L., Stone, S. R., Chang, W. S., and Carrell, R. W. (1993) *Biochemistry 32*, 500−508.
5. Lomas, D. A., Finch, J. T., Seyama, K., Nukiwa, T., and Carrell, R. W. (1993) *J. Biol. Chem. 268*, 15333−15335.
6. Lomas, D. A., Elliott, P. R., Sidhar, S. K., Foreman, R. C., Finch, J. T., Cox, D. W., Whisstock, J. C., and Carrell, R. W. (1995) *J. Biol. Chem. 270*, 16864−16870.
7. Beauchamp, N. J., Pike, R. N., Daly, M., Butler, L., Makris, M., Dafforn, T. R., Zhou, A., Fitton, H. L., Preston, F. E., Peake, I. R., and Carrell, R. W. (1998) *Blood 92*, 2696−2706.
8. Davis, R. L., Shrimpton, A. E., Holohan, P. D., Bradshaw, C., Feiglin, D., Collins, G. H., Sonderegger, P., Kinter, J., Becker, L. M., Lacbawan, F., Krasnewich, D., Muenke, M., Lawrence, D. A., Yerby, M. S., Shaw, C. M., Gooptu, B., Elliott, P. R., Finch, J. T., Carrell, R. W., and Lomas, D. A. (1999) *Nature 401*, 376−379.
9. Elliott, P. R., Bilton, D., and Lomas, D. A. (1998) *Am. J. Respir. Cell. Mol. Biol. 18*, 670−674.
10. Koloczek, H., Banbula, A., Salvesen, G. S., and Potempa, J. (1996) *Protein Sci. 5*, 2226−2235.
11. James, E. L., and Bottomley, S. P. (1998) *Arch. Biochem. Biophys. 356*, 296−300.
12. James, E. L., Whisstock, J. C., Gore, M. G., and Bottomley, S. P. (1999) *J. Biol. Chem. 274*, 9482−9488.
13. Dafforn, T. R., Mahadeva, R., Elliott, P. R., Sivasothy, P., and Lomas, D. A. (1999) *J. Biol. Chem. 274*, 9548−9555.
14. Yu, M. H., Lee, K. N., and Kim, J. (1995) *Nat. Struct. Biol. 2*, 363−367.
15. Bruch, M., Weiss, V., and Engel, J. (1988) *J. Biol. Chem. 263*, 16626−16630.
16. Lawrence, D. A., Ginsburg, D., Day, D. E., Berkenpas, M. B., Verhamme, I. M., Kvassman, J. O., and Shore, J. D. (1995) *J. Biol. Chem. 270*, 25309−25312.
17. Huntington, J. A., Read, R. J., and Carrell, R. W. (2000) *Nature 407*, 923−926.
18. Stratikos, E., and Gettins, P. G. (1999) *Proc. Natl. Acad. Sci. U.S.A. 96*, 4808−4813.
19. Tew, D. J., and Bottomley, S. P. (2001) *FEBS Lett. 494*, 30−33.
20. Peterson, F. C., and Gettins, P. G. (2001) *Biochemistry 40*, 6284−6292.
21. Herve, M., and Ghelis, C. (1990) *Eur. J. Biochem. 191*, 653−658.
22. Powell, L. M., and Pain, R. H. (1992) *J. Mol. Biol. 224*, 241−252.
23. Tew, D. J., and Bottomley, S. P. (2001) *J. Mol. Biol. 313*, 1163−1171.
24. Perry, D. J., Marshall, C., Borg, J. Y., Tait, R. C., Daly, M. E., Walker, I. D., and Carrell, R. W. (1995) *Blood Coagulation Fibrinolysis 6*, 51−4.
25. Sui, G. C., Mangs, H., and Wiman, B. (1999) *Biochim. Biophys. Acta 1434*, 58−63.
26. Vleugels, N., Gils, A., Bijnens, A., Knockaert, I., and Declerck, P. J. (2000) *Biochim. Biophys. Acta 1476*, 20−26.
27. Gooptu, B., Hazes, B., Chang, W. S., Dafforn, T. R., Carrell, R. W., Read, R. J., and Lomas, D. A. (2000) *Proc. Natl. Acad. Sci. U.S.A. 97*, 67−72.
28. Bijnens, A. P., Gils, A., Knockaert, I., Stassen, J. M., and Declerck, P. J. (2000) *J. Biol. Chem. 275*, 6375−6380.
29. Wind, T., Jensen, M. A., and Andreasen, P. A. (2001) *Eur. J. Biochem. 268*, 1095−1106.
30. Zhou, A., Carrell, R. W., and Huntington, J. A. (2001) *J. Biol. Chem. 276*, 27541−27547.
31. Djie, M. Z., Lebonniec, B. F., Hopkins, P. C. R., Hipler, K., and Stone, S. R. (1996) *Biochemistry 35*, 11461−11469.
32. Stone, S. R., and Le Bonniec, B. F. (1997) *J. Mol. Biol. 265*, 344−362.
33. Bottomley, S. P., and Chang, W.-S. (1997) *Biochem. Biophys. Res. Commun. 241*, 264−269.
34. Pace, C. N. (1986) *Methods Enzymol. 131*, 266−280.
35. Pearce, M. C., Rubin, H., and Bottomley, S. P. (2000) *J. Biol. Chem. 275*, 28513−28518.
36. Bolen, D. W., and Santoro, M. M. (1988) *Biochemistry 27*, 8069−8074.
37. Santoro, M. M., and Bolen, D. W. (1988) *Biochemistry 27*, 8063−8068.
38. Nath, U., and Udgaonkar, J. B. (1995) *Biochemistry 34*, 1702−1713.
39. Lehrer, S. S. (1971) *Biochemistry 10*, 3254−3263.
40. Huntington, J. A., Pannu, N. S., Hazes, B., Read, R. J., Lomas, D. A., and Carrell, R. W. (1999) *J. Mol. Biol. 293*, 449−455.
41. Dunstone, M. A., Dai, W., Whisstock, J. C., Rossjohn, J., Pike, R. N., Feil, S. C., Le Bonniec, B. F., Parker, M. W., and Bottomley, S. P. (2000) *Protein Sci. 9*, 417−420.
42. Whisstock, J., Skinner, R., and Lesk, A. M. (1998) *Trends Biochem. Sci. 23*, 63−67.
43. Irving, J. A., Pike, R. N., Lesk, A. M., and Whisstock, J. C. (2000) *Genome Res. 10*, 1841−1860.
44. Elliott, P. R., Abrahams, J. P., and Lomas, D. A. (1998) *J. Mol. Biol. 275*, 419−425.
45. Whisstock, J. C., Skinner, R., Carrell, R. W., and Lesk, A. M. (2000) *J. Mol. Biol. 295*, 651−665.
46. Li, J., Wang, Z., Canagarajah, B., Jiang, H., Kanost, M., and Goldsmith, E. J. (1999) *Structure 7*, 103−109.
47. Dong, A., Meyer, J. D., Brown, J. L., Manning, M. C., and Carpenter, J. F. (2000) *Arch. Biochem. Biophys. 383*, 148−155.
48. Lakowicz, J. R. (1999) *Principles of Fluorescence Spectroscopy*, 2nd ed., Plenum Publishers, New York.
49. Smith, C. J., Clarke, A. R., Chia, W. N., Irons, L. I., Atkinson, T., and Holbrook, J. J. (1991) *Biochemistry 30*, 1028−1036.
50. Bottomley, S. P., Popplewell, A. G., Scawen, M., Wan, T., Sutton, B. J., and Gore, M. G. (1994) *Protein Eng. 7*, 1463−1470.
51. Clark, P. L., Liu, Z. P., Zhang, J., and Gierasch, L. M. (1996) *Protein Sci. 5*, 1108−1117.
52. Clark, P. L., Weston, B. F., and Gierasch, L. M. (1998) *Folding Des. 3*, 401−412.
53. Shao, X., and Matthews, C. R. (1998) *Biochemistry 37*, 7850−7858.
54. Fish, W. W., Danielsson, A., Nordling, K., Miller, S. H., Lam, C. F., and Bjork, I. (1985) *Biochemistry 24*, 1510−1517.
55. Sivasothy, P., Dafforn, T. R., Gettins, P. G., and Lomas, D. A. (2000) *J. Biol. Chem. 275*, 33663−33668.
56. Mellet, P., and Bieth, J. G. (2000) *J. Biol. Chem. 275*, 10788−10795.
57. O'Malley, K. M., and Cooperman, B. S. (2000) *J. Biol. Chem. 276*, 6631−6639.
58. O'Malley, K. M., Nair, S. A., Rubin, H., and Cooperman, B. S. (1997) *J. Biol. Chem. 272*, 5354−5359.
59. Kraulis, P. J. (1991) *J. Appl. Crystallogr 24*, 946−950.
60. Nath, U., and Udgaonkar, J. B. (1995) *Biochemistry 34*, 1702−1713.

BI0158932